Int. J. Therm. Sci. (2000) 39, 1028–1038

S1290-0729(00)01190-X/FLA

Axial dispersion in shell-and-tube heat exchangers *

Wilfried Roetzel **, Frank Balzereit

Institut für Thermodynamik, Universität der Bundeswehr Hamburg, D-22039 Hamburg, Germany

(Received 5 May 2000, accepted 27 July 2000)

Dedicated to Prof. Dr.-Ing. Dr. h.c. mult. Karl Stephan on the occasion of his 70th birthday

Abstract — The effect of the deviation of the actual three-dimensional flow field on the shell-side from the frequently assumed one-dimensional uniform axial plug flow can be taken into account by superimposed axial dispersion in the fluid. The measure for axial dispersion is the Péclet number which can vary from infinite (no dispersion) to zero (complete axial mixing). For the fast and more reliable calculation of transient processes with the axial dispersion model, the Péclet number has to be known. A residence time distribution measurement technique for the determination of shell-side dispersive Péclet numbers is described and used to determine Péclet numbers for different shell-to-baffle clearances, numbers of baffles, and axial plug flow Reynolds numbers. Measurements with water reveal that Péclet numbers from 15 to 160 can occur and axial dispersion cannot be neglected in many cases. © 2000 Éditions scientifiques et médicales Elsevier SAS

shell-and-tube / heat exchanger / axial dispersion / residence time distribution

Résumé — **Dispersion axiale dans des échangeurs tubulaires à faisceau et calandre.** L'effet de la déviation de l'écoulement tridimensionnel coté calandre de l'écoulement axial uniforme unidimensionnel fréquemment assumé peut être pris en considération par une dispersion axiale superposée dans le fluide. La mesure pour la dispersion axiale est le nombre de Péclet qui peut changer d'infini (aucune dispersion) à zéro (mélange axial complet). Pour le calcul rapide et fiable des processus en régime transitoire avec le modèle de dispersion axial, le nombre de Péclet doit être connu. Une technique de mesure de distribution de temps de séjour pour la détermination des nombres de Péclet dispersif coté calandre est décrite et utilisée pour déterminer des nombres de Péclet en relation avec l'écart entre les chicanes et la calandre, le nombre de chicanes et le nombre de Reynolds. Les mesures avec de l'eau indiquent que les nombres de Péclet de 15 à 160 peuvent se produire et la dispersion axiale ne peut pas être négligée dans beaucoup de cas. © 2000 Éditions scientifiques et médicales Elsevier SAS

tubulaire à faisceau et calandre / échangeur de chaleur / dispersion axiale / distribution de temps de séjour

Nomenclature

a	apparent thermal diffusivity (with subscript W molecular value)	$m^2 \cdot s^{-1}$
b	dimensionless root of eigenfunction, equation (13)	
c	dimensionless concentration defined by equation (7)	
c^*, C^*	steady-state dimensionless concentrations	
$\bar{c}$	dimensionless concentration in the Laplace domain	
C	concentration	$kg \cdot m^{-3}$
d	equivalent diameter; outer diameter of tubes in bundle	m
D	mass dispersion coefficient	$m^2 \cdot s^{-1}$
	diameter of heat exchanger shell	m
E	residence time distribution function . .	s^{-1}
f	dimensionless inlet concentration function	
$\bar{f}$	inlet concentration function in the Laplace domain	
F	heat transfer area	m^2
L	flow length of test section	m
L	Laplace transform function	
n	number of tubes in the bundle	
NTU	number of transfer units	
$Pe_{a,D}$	dispersive Péclet number for the fluid defined by equations (4a) and (8a)	
Pe_W	nondispersive Péclet number for the wall defined by equation (4b)	

* Presented at the International Conference "Heat Exchangers for Sustainable Development", June 15–18, 1998, Lisbon, Portugal.

** Correspondence and reprints.
Wilfried.Roetzel@unibw-hamburg.de

Re	axial plug-flow Reynolds number defined by equation (19)	
s	Laplace parameter	s^{-1}
t	dimensionless time defined by equation (3b)	
T	thermodynamic temperature	K
V	volume of the test section	m^3
$\dot{V}$	volumetric flow rate	$m^3 \cdot s^{-1}$
w	velocity	$m \cdot s^{-1}$
$\dot{W}$	heat capacity rate	$W \cdot K^{-1}$
x	dimensionless flow length defined by equation (3a)	
x_p	dimensionless calibration factor of the electrical conductivity probe	
x_T	dimensionless calibration factor of temperature defined by equation (17)	
X	flow length	m

Greek symbols

α	heat transfer coefficient	$W \cdot m^{-2} \cdot K^{-1}$
δ	Dirac pulse function	
Λ_p	electrical conductivity of the probe	S
ν	kinematic viscosity	$m^2 \cdot s^{-1}$
τ	time	s
$\bar{\tau}$	mean time	s
$\bar{\tau}_R$	mean system residence time	s

Subscripts

a	thermal dispersion
ax	axial
D	mass dispersion
eqv	equivalent
in	inlet
i	run parameter
j	run parameter
m	taken at mean of parameters
n	run parameter
out	outlet
tot	total (whole test section)
W	wall

1. INTRODUCTION

Various methods of different complexity are available for the thermal design and rating of shell-and-tube heat exchangers. The simple and fast methods, applying the concept of mean temperature difference and number of transfer units, are based on the plug flow model in which both streams are assumed to flow with uniform velocity in the axial direction. Particularly on the shell-side, the real flow field is very complex and the traditional plug flow model is unrealistic [1, 2].

The traditional plug flow model can be improved by introducing an apparent axial heat conduction or dispersion term into the energy equation of the fluid which leads to the axial dispersion model. With an appropriate value of the apparent conductivity or dispersion coefficient all deviations from the ideal plug flow — such as cross-flow between baffles, bypassing around the bundle, leakage flows between baffles and shell and tubes, stagnant flows and mixing — are taken into account. The axial dispersion model was first suggested by Taylor [3] for mass dispersion in turbulent pipe flow and is applied and further developed for heat exchangers since the end of the eighties [4, 5]. Especially for the calculation of transient processes in heat exchangers and thermal regenerators the axial dispersion model has proven to be a suitable tool and the simple but reliable alternative to prohibitively time consuming numerical calculations [6, 7]. For the application of the model the axial dispersion coefficient or in dimensionless form the dispersive Péclet number Pe has to be known. This parameter is a flow property and depends on the flow regime and the geometry of the flow channel in the exchanger.

The theoretical prediction of the dispersive Péclet number is too complicated for the shell-side flow channel and measurements are necessary for its determination. Various transient or periodic measurement techniques have been developed and tested for the simultaneous determination of the dispersion coefficient and heat transfer coefficient [8, 9].

These thermal methods have the advantage that one single experiment yields two consistent values of NTU and Pe which are both needed for the calculation of transient processes in the exchanger.

On the other hand, the simultaneous estimation of two unknowns is disadvantageous because the accuracy could be too low in some regions of parameters. It would, therefore, be useful, if one of both unknowns could be measured in an additional experiment. If the Péclet number would be measured separately the heat transfer coefficient (NTU) could be determined with high accuracy with one of the thermal methods.

A suitable method for obtaining the Péclet number alone seems to be the most recently developed salt pulse technique [10]. The analogy of heat and mass transfer for the process of dispersion allows the prediction of the thermal Péclet number with a mass dispersion experiment. The dispersive Péclet number is determined through residence time distribution measurements. Water flows with constant velocity through the shell-side flow channel. In front of the channel a salt solution pulse is injected into the flow stream which propagates with dispersion to the

exit. Before the entry and behind the exit the salt concentration profiles are measured as a function of time using a newly developed detector system for fast changes in concentration [11]. The evaluation of both profiles yields the unknown Péclet number. Residence time measurements are carried out on the shell-side of an exchanger with variable shell-to-baffle clearance (0.2, 1.0, and 3.0 mm) and spacing of the baffles (7, 11, 17, and 25 baffles). More details about the measurement technique, the model and its boundary conditions are given by Balzereit [12]. It should be mentioned that some derivations and explanations, which have been presented in the previous paper of the same authors [10], are repeated in this paper for better understanding.

2. ANALYSIS OF AXIAL DISPERSION MODEL

The one-dimensional transient energy equation for plug flow and longitudinal (axial) dispersion expressed in analogy to Fourier's law of heat conduction

$$\frac{\partial T}{\partial t} + \frac{\partial T}{\partial x} = \frac{1}{Pe_a}\frac{\partial^2 T}{\partial x^2} + NTU(T_W - T) \tag{1}$$

describes the transport of heat in a single incompressible fluid stream in the heat exchanger. It is coupled with the energy equation for the wall

$$\frac{\partial T_W}{\partial t} = \frac{1}{Pe_W}\frac{\partial^2 T_W}{\partial x^2} - NTU(T_W - T) \tag{2}$$

Dimensionless quantities are used for flow length

$$x = \frac{X}{L} \tag{3a}$$

time

$$t = \tau\,\frac{w}{L} = \tau\,\frac{\dot V}{V} \tag{3b}$$

dispersion coefficients

$$Pe_a = \frac{wL}{a} \tag{4a}$$

and

$$Pe_W = \frac{wL}{a_W} \tag{4b}$$

and heat transfer coefficient

$$NTU = \frac{\alpha F}{\dot W} \tag{5}$$

Pe_a is formed with the apparent thermal diffusivity in the observed fluid stream, while Pe_W is a nonconvective coefficient formed with the real thermal diffusivity of the wall.

For an adiabatic wall condition $\alpha = 0$ and $NTU_\alpha = 0$ the coupling of the fluid and wall equations is elevated, hence, only the equation for the observed fluid stream flowing in an adiabatic channel needs to be considered. Applying the analogy for heat and mass dispersion and, hence, replacing temperature by mass concentration one obtains the transient mass transport equation for a passive tracer:

$$\frac{\partial c}{\partial t} + \frac{\partial c}{\partial x} = \frac{1}{Pe_D}\frac{\partial^2 c}{\partial x^2} \tag{6}$$

with the dimensionless concentration

$$c = \frac{C}{C^*}, \quad \text{formed with } C^* = \frac{\int_0^\infty C_{out}\,\mathrm{d}\tau}{\bar\tau_R} \tag{7}$$

The Péclet number for mass dispersion

$$Pe_D = \frac{wL}{D} \tag{8a}$$

is equal to the Péclet number for heat dispersion (equation (4a)) if the analogy of heat and mass dispersion holds true:

$$a = D \quad \rightarrow \quad Pe_a = Pe_D = Pe \tag{8b}$$

The proof of this analogy is subject to separate investigations. Preliminary experiments confirm equation (8b).

The characteristic length L is the plug flow length of an equivalent model of the real system, which is covered by the fluid flowing with the average velocity w for a time period equal to the mean system residence time.

The initial and boundary conditions are according to Danckwerts [13]

$$t = 0,\ 0 \le x \le 1: \quad c = 0 \tag{9a}$$

$$t > 0,\ x = 0:$$

$$c_{0^+} - \frac{1}{Pe}\frac{\partial c_{0^+}}{\partial x} = c_{0^-} = f(t) \quad \text{and} \tag{9b}$$

$$t > 0,\ x = 1: \qquad \frac{\partial c_{1^-}}{\partial x} = 0 \tag{9c}$$

The rate at which mass transfer occurs across the plane at $x = 0$ by combined convective flow and dispersion must be equal to the rate at which mass is transported to the system [13]. The result is a sudden drop of concentration at the inlet even at steady-state mass transport to the system, hence, $f(t) = c^*$. This is characteristic of a closed system with negligible dispersion outside the

system boundaries, and is obviously a realistic condition for heat exchangers connected to tubes with turbulent (plug) flow. The function $f(t)$ can be any transient function for the concentration at the system inlet.

Taking the Laplace transform of equation (6) and the boundary conditions (9) with respect to t one obtains an ordinary differential equation

$$\frac{1}{Pe}\frac{\mathrm{d}^2\bar{c}}{\mathrm{d}x^2} - \frac{\mathrm{d}\bar{c}}{\mathrm{d}x} = s\bar{c} \tag{10}$$

and boundary conditions

$$x = 0: \quad \bar{c} - \frac{1}{Pe}\frac{\mathrm{d}\bar{c}}{\mathrm{d}x} = L\big[f(t)\big] = \bar{f}(s) \quad \text{and} \tag{11a}$$

$$x = 1: \quad \frac{\mathrm{d}\bar{c}}{\mathrm{d}x} = 0 \tag{11b}$$

Equation (10) and the boundary conditions (11) are solved in the Laplace domain and the solution is inversely transformed by the method of residues [10, 14].

In the experiments a pulse of tracer substance is injected into the fluid flow. Separate calculations show that the pulse can be regarded as a Dirac pulse at the inlet boundary $x = 0$: $f(t) = \delta(t)$, and hence we get: $\bar{f}(s) = 1$.

The system outlet response ($x = 1$) to a Dirac pulse input at time $t = 0$ represents the distribution of fluid residence times (RTD)

$$E(t) = \sum_{j=1}^{\infty} \frac{b_j^2[2\cos(b_j) + (Pe/b_j)\sin(b_j)]}{b_j^2 + Pe^2/4 + Pe} \cdot \mathrm{e}^{Pe/2-(Pe/4+b_j^2/Pe)t} \tag{12}$$

where $b_j \in \mathbb{R}$ are determined from

$$\tan b_j = \frac{Pe\, b_j}{b_j^2 - Pe^2/4} \quad \text{for } j = 1, 2, \ldots, \infty \tag{13}$$

3. MEASUREMENT PRINCIPLE

3.1. Evaluation of residence time distribution measurements

Our concern is with the evaluation of the dispersion coefficient which is characterized by the distribution of fluid residence times. We consider an incompressible fluid flow with constant properties throughout the exchanger and, hence, observe a mathematically linear system. The simplest way to proceed is to follow a sharp initial pulse of (nondiffusing) tracer moving through the system with the fluid, and base description of the flow conditions in the exchanger on it. In a linear system with constant system properties, the distribution of tracer at the outlet can be expressed as a linear functional of the inlet concentration [15]:

$$c_{\mathrm{out}}(\tau) = \int_0^{\tau} E\big(\tau^*\big)c_{\mathrm{in}}\big(\tau - \tau^*\big)\,\mathrm{d}\tau^* \tag{14}$$

The analytical residence time distribution function $E(\tau)$ explicitly obtained by integration of the flow equation, containing the properties of the axial dispersion model, combined with the experimental input signal $c_{\mathrm{in}}(\tau)$ in the convolution integral will yield the calculated system response signal $c_{\mathrm{out}}(\tau)$. This calculated response can be fitted to the measured outlet signal to acquire an optimum value of the dispersion coefficient.

For an inlet concentration $c_{\mathrm{in}}(\tau) = \delta(\tau)$, $E(\tau) = c_{\mathrm{out}}(\tau)$ is the desired distribution of residence times and the analytical $E(\tau)$ can be fitted directly to the measured outlet signal. This is permissible for inlet signals whose duration in time for entry is much smaller than the mean residence time. Evaluations of measurements with inlet signal time to mean residence time of up to 3 % have shown negligible effect on the shape of the calculated response curve in the observed range of dispersion coefficients in the shell-and-tube heat exchanger ($Pe =$ 15–160).

For comparison of the response signals, the measured time-scale needs to be normalized by relating it to the mean fluid residence time. The individual residence times of all tracer particles give a distribution of residence times, which can be characterized by the residence time density $E(\tau)\,\mathrm{d}\tau$. It is defined as the fraction of fluid with a residence time within $\mathrm{d}\tau$ of τ. If one looks at $E(\tau)$ as the output response of a linear system to a pulse input, the concept of temporal moments yields

$$1 \equiv \int_0^{\infty} E(\tau)\,\mathrm{d}\tau \quad \text{and} \quad \bar{\tau} = \int_0^{\infty} \tau E(\tau)\,\mathrm{d}\tau \tag{15}$$

where $\bar{\tau}$ is the mean of the residence time distribution. It is obtained as the arithmetic average of all fluid particle (individual) residence times weighted with the fraction of particles with this particular residence time. For an arbitrary input signal introduced upstream of an observed system the mean residence time of this system is obtained as the difference of the means of the signals at the outlet and the inlet

$$\bar{\tau}_{\mathrm{R}} = \bar{\tau}_{\mathrm{out}} - \bar{\tau}_{\mathrm{in}} \tag{16}$$

The calculation of $\bar{\tau}_R$ from the experimental distribution function, however, is sensitive to the disproportionately large weighting given to the tails of the shape of $c_{out}(\tau)$, the tails having typically a higher uncertainty in values. It is advisable to use a second method applicable here for comparison.

Knowing the volumetric flow rate $\dot{V}$ and volume V of a closed system, i.e. the exchanger, the average residence time for fluid particles can be calculated as $\bar{\tau}_R = V/\dot{V}$ for steady incompressible flow, if transport across the system boundaries is due to convection only, hence, diffusion is negligible, and the pulse of passive tracer material is injected uniformly across the inlet [16]. Velocities and effective diffusion coefficient have to be independent of concentration. For the shell-and-tube heat exchanger under investigation these conditions are met because plug flow can be assumed in the connected tubes at turbulent flow and a uniform distribution of concentration over the outlet cross-section was detected using three probes. Therefore, negligible dispersion outside the boundaries of the exchanger is present. Furthermore, dispersion is a flow property assumed to be independent of concentration gradients of the tracer substance which is only used to mark fluid particles. The effect of molecular diffusion under these turbulent flow conditions is negligible.

3.2. Transient concentration measurement technique

A measurement technique was developed by Köllmann and Balzereit [11] which allows accurate detection of fast concentration changes of an electrolyte solution in a flow cross-section. The technique is based on the quick determination of electrical conductivity by scanning electrical AC signals on conductivity probes, placed in the electrolyte solution, in discrete time and amplitude steps and processing them digitally. Time resolution of less than 1 ms is achieved having an uncertainty of less than 1 % of the amplitude measured, the latter valid over two decades in order of magnitude for each measuring range. The measurement technique has been tested in an electrical conductivity range of 0.02 to 200 mS.

Concentration values are obtained from the measured electrical conductivity by calibration. Various geometries of conductivity probes for different measurement situations can be used, resulting only in different geometric factors and probe impedances. Impedances of the conductivity measuring device are taken into account during the conductivity measurement. Probe geometry and temperature of the solution to be measured determine conversion factors for concentration measurement. A highly linear relationship between electrical conductivity and concentration at constant temperature is valid for lower concentrations as were observed at the outlet of the test section. Nonlinearities occurring at higher concentrations can be included through calibration. Prausnitz and Wilhelm [17] noted and experiments show that the flow rate does not effect the measured conductivity or concentration values. Uncertainty in concentration of less than 2 % is achieved by calibration in the running experimental setup.

Electrical insulation of the fluid system in which measurements are to take place allows the use of very simple conductivity probes. With selection of a distinct (under-) sampling rate for scanning the signals high resolution measurements of adequately averaged signals can be obtain using inexpensive A/D converters.

The increase of electrical conductivity of a solution of constant concentration with a rise in temperature can be accounted for by a factor which is linearly dependent on the thermodynamic temperature T:

$$x_T = a\,\frac{T}{293.15\ \mathrm{K}} + b \tag{17}$$

where a and b are constants and found to be $a = 6.1547$ and $b = -5.1547$ for pure NaCl solutions.

The following functional relationship between the electrical conductivity Λ_P and concentration C was found for each of the probes used:

$$\Lambda_P(C,T) = x_P x_T f(C) \tag{18}$$

where x_P is a constant geometric factor of the probe and $f(C)$ is a function of concentration only (linear for not too high concentrations) for all probe geometries [11]. The impedances of the probe have to be measured and their values inserted into the running program. They only have an impact at very low concentrations, which can be noticed as the calibration curve intersects the line of zero concentration at a value for conductivity slightly above zero.

According to equation (18) the detector can also be used as an inertia-free thermometer for the fluid temperature.

4. EXPERIMENTS

4.1. Shell-and-tube heat exchanger

Experiments were carried out on the shell-side of a variable shell-and-tube heat exchanger (sketch in *fig-*

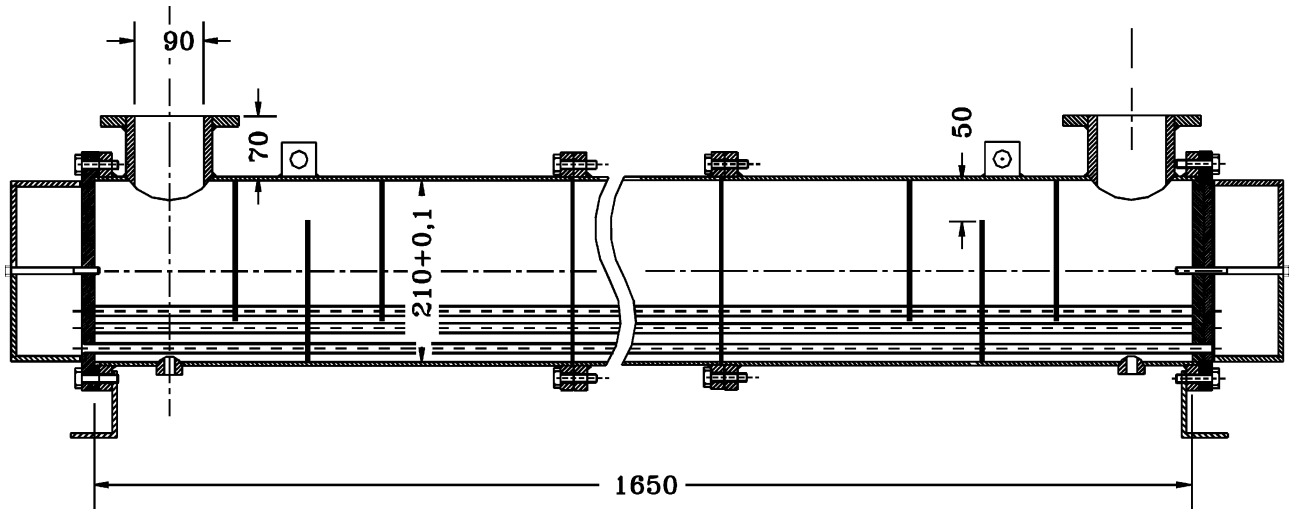

Figure 1. Sketch of the shell-and-tube heat exchanger used in experiments.

ure 1) with one tubeside and one shellside pass, and which has been operated with different spacing of the baffles (7, 11, 17, and 25 baffles) and shell-to-baffle clearance (0.2, 1.0, and 3.0 mm). The inner diameter of the shell is 210 mm. The tube bundle consists of 92 steal tubes with 12 mm outer diameter, and an effective length for heat transfer of 1 650 mm. The pitch ratio is 1.5. The above-mentioned number of baffles (each 2 mm thick) corresponds to a constant distance between each of the baffles of 219, 130, 81.1, and 53.7 mm, respectively. The largest open window between each of the baffles and the shell wall is 50 mm (24 % of the shell inner diameter). The connection nozzles have an inner diameter of 90 mm.

To vary the shell-to-baffle clearance different sets of baffles had to be used. Of the twelve possible combinations of baffle spacing and clearance all where investigated.

The tube-to-baffle clearance is only 0.1 mm, and hence, after short duration of operation most likely clogged and should not allow any significant bypass.

The shell-side volumetric flow rate using water of 20 to 30 °C was varied for all configurations between 30 and 210 $l \cdot min^{-1}$ (0.5 to 3.5 $l \cdot s^{-1}$). The Reynolds number used for evaluation and representation of the measured data is the "axial plug flow Reynolds number"

$$Re = \frac{w_{ax} d_{eqv}}{\nu_m} = \frac{4\dot{V}_{tot}}{\pi(nd + D)\nu_m} \qquad (19)$$

with ν_m the kinematic viscosity evaluated at the mean temperature of the fluid.

Measurements of the residence time distribution (RTD) were carried out on the shell-side of the exchanger with a constant fluid temperature ($\Delta T < 0.3$ K) and volumetric flow rate in the apparatus for the duration of each measurement.

4.2. Experimental setup and procedure

The experimental setup to inject a salt solution pulse into the inlet flow stream of the shell-side of the heat exchanger and to measure the response at the outlet is shown in *figure 2*. It consists of the components:

- shell-and-tube heat exchanger (S&THE),
- device for injection of a pulse like tracer signal,
- device for measurement of fast concentration changes by probing electrical conductivity at the inlet and outlet of the test section/S&THE,
- flow rate meter and thermoelements for observing the steady and almost isothermal flow.

Desalted water (with electrical conductivity < 0.2 $mS \cdot cm^{-1}$) flows at a constant flow rate through the heat exchanger in a closed loop system. The flow rate is measured with a calibrated turbine flow meter. The temperature is measured with type K thermocouples at the inlet and outlet of the exchanger. Salt solution (NaCl of approximate concentration 200 $g \cdot l^{-1}$) is prepared in a vessel at a pressure of 600 kPa. Six magnetic valves are

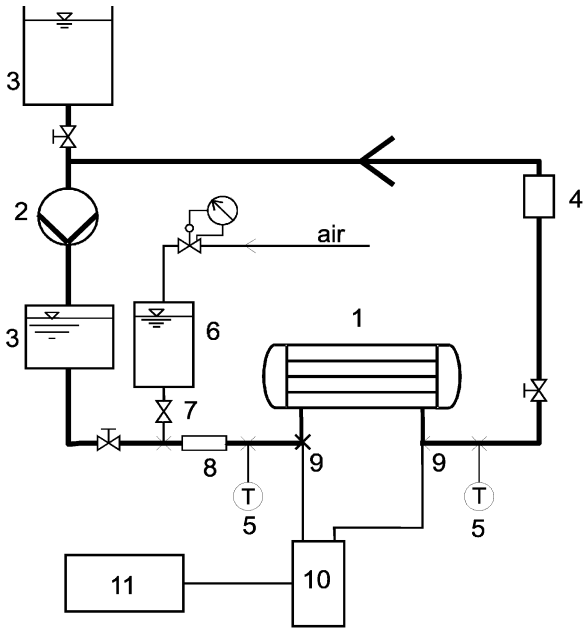

1. shell-and-tube heat exchanger 2. pump 3. tank
4. turbine flowmeter 5. thermoelement 6. electrolyte solution reservoir 7. magnetic valve 8. packed bed
9. conductivity probes 10. signal generator
11. A/D converter and PC

Figure 2. Overall experimental setup.

supplied with the salt solution on one side and are located at 90° angles in circular arrangement around the inlet tube about 1.5 internal diameters in front of the exchanger inlet, extending each with a nozzle into the flow stream. In the starting position they retain the salt solution from entering the main flow stream. The valves are controlled by a monostable timer to synchronically open for a short pulse duration of approximately 80–100 ms.

Electrical conductivity probes are located at the beginning and the end of the test section, the inlet and outlet of the exchanger, respectively. They consist of two electrodes made from 0.5 mm platinum wire with one electrode of a short tip in the center of the probe and the second one, which is grounded, is coiled around it, providing an optimum geometry for shielding the inner electrode [18]. The probes are well protected from influences of external electrical fields and especially the currents introduced by the other electrodes in the fluid.

Using common hardware components (PC and ADC) and an appropriate sampling rate successive averaged measurements of the electrical conductivity of the fluid in the inlet and exit cross-section where obtained every 10–50 ms with an uncertainty of less than 2 % for all concentrations larger than approximately 2 % of the average response peaks.

At the beginning of the experiment the monostable timer is started which supplies sufficient voltage to the magnetic valves for an adjustable length of time, the valves open and close again simultaneously, and a salt solution pulse is injected into the flow stream. The inlet conductivity probe detects the fast concentration change of the electrolyte solution as it has reasonably well mixed with the flow stream before it reaches the conductivity probe at the inlet of the test section.

The objective is to realize an ideal pulse as closely as possible for a system input while injecting enough salt to get a strong enough output response for a good quality evaluation. The pulse length of about 100–500 ms used in the experiments allows short enough injection pulses of about 1–2 % of the mean system residence time for the responses to satisfy well an idealized pulse-response evaluation. Another advantage of a short pulse input is the fact that a precise registration of the average concentration of the fluid passing the inlet cross-section area is not necessary. Deviations between the measured and the actual concentration profile entering the system due to incomplete mixing of the injected solution and the desalted main flow stream at the conductivity probe have negligible effect on the shape of the exit stream concentration profile. Measurements with a packed bed between injection point and inlet probe to enhance radial mixing have been observed for comparison.

Measurements were conducted at constant flow rates between 30 and 210 $\mathrm{l \cdot min^{-1}}$, estimated to be constant and accurately measured within 2 %. The accuracy of the calibrated thermocouples is 0.1 K with water temperatures between 20 and 30 °C. The temperature, increasing slowly through dissipation, stayed constant and equal within 0.1 K on both sides of the exchanger during each experiment.

4.3. Evaluation

The measured conductivity values are converted into concentration values according to the temperature-dependent calibration function derived from equation (18). Concentration profiles of the measured inlet-signal and the exit-response as a function of time are obtained. The experimental outlet curve is then converted to dimensionless time and concentration values by relating the time to the mean time of the inlet signal and the system residence time, hence, $t = (\tau_{\mathrm{out}} - \bar{\tau}_{\mathrm{in}})/\bar{\tau}_{\mathrm{R}}$, and the concentration to

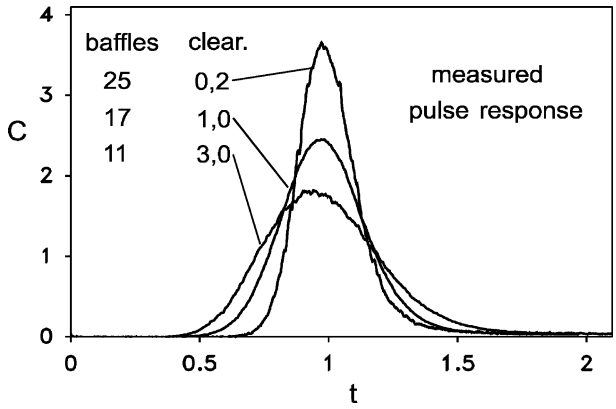

Figure 3. Representative measured dimensionless pulse responses of the S&THE; with number of baffles/shell-to-baffle clearances: 25/0.2 mm; 17/1.0 mm; 11/3.0 mm.

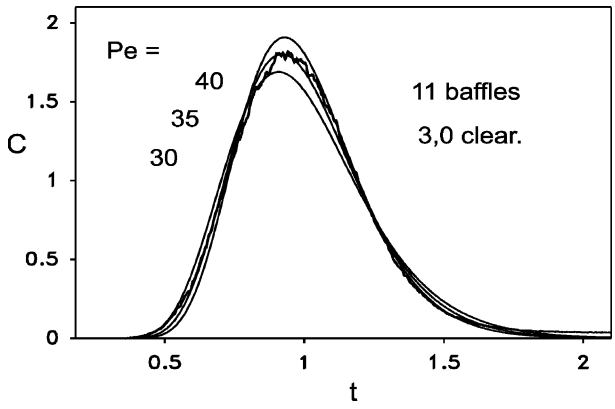

Figure 4. Measured and calculated system response to the experimental inlet signal for S&THE with 11 baffles and 3.0 clearance, $Pe = 35$, $Re = 3300$; dimensionless concentration c as a function of dimensionless time t.

the total amount of tracer and the mean residence time according to equation (7).

For determining the dispersion coefficient, the experimental response profile at the exchanger outlet is compared to the calculated (analytical) response of the dispersion model to the experimental inlet signal (equations (12) and (14)). The mean residence time is determined by measurement of the flow rate and volume as well as the difference of the first normalized moments of the RTD (equations (15) and (16)); the values agreed mostly to within 3 %. Direct observation of the curve fit permits judgment about the applicability of the model and control over the quality of the measurement.

Measured pulse responses of three representative experiments are shown in *figure 3*. An example of an experimental curve and the optimum fit to the dispersion model is presented in *figure 4*. The resulting values for the Péclet number as a function of the Reynolds number are shown in *figures 5a–d* and *6*. The parameter in *figures 5a–d* is the shell-to-baffle clearance for a fixed number of baffles for each graph. In *figure 6* the values of the Péclet number for varying number of baffles are shown for a relatively large clearance of 3.0 mm. *Figure 7* presents the evident effect of baffle spacing and clearance on the axial dispersion coefficient for a fixed axial plug-flow Reynolds number.

4.4. Results and discussion

Comparison of the measured and the analytical model response to a pulse input confirm well the applicability of describing the overall system flow characteristics with the dispersion model. Allowing for a 2 % inaccuracy for the measured concentration profiles and a 2 % uncertainty for the mean residence time of the fluid observed, most Péclet numbers are determined with an accuracy of 3–10 % depending on the range. Individual measurements, most likely due to experimental mistakes, can leave this range of accuracy. The one parameter that will have the most significant effect on the shape of the measured curve when it is converted to the dimensionless scales of time and concentration is the location of the mean residence time in relation to the experimental curve. The uncertainty about this value should not exceed 2 %. Longer tails in the concentration profile, as mostly observed in systems with large dispersion (small Péclet numbers), introduce larger uncertainties when the mean residence time is determined from the first temporal moment of the distribution. Hence, basing evaluation on the measured distribution as well as measurement of system volume and flow rate will reduce the chances for systematic errors.

Figures 5a–d present measured data points and a linear fit for the dependence of the Péclet number on the axial plug flow Reynolds number for each investigated configuration of the shell-and-tube heat exchanger. There is a slight increase in Péclet number with Reynolds number for most configurations with different numbers of baffles installed and different shell-to-baffle clearance except for 7 and 17 baffles with 0.2 mm clearance. The relative increase is not the same for all or relative to the number of baffles. For any apparatus the dependence is monotonic. For each number of baffles the range of the Péclet numbers is higher for smaller shell-to-baffle clearance due to the decreasing effect of bypass streams. The same increase in the Péclet number takes place when comparing equal values for the shell-to-baffle

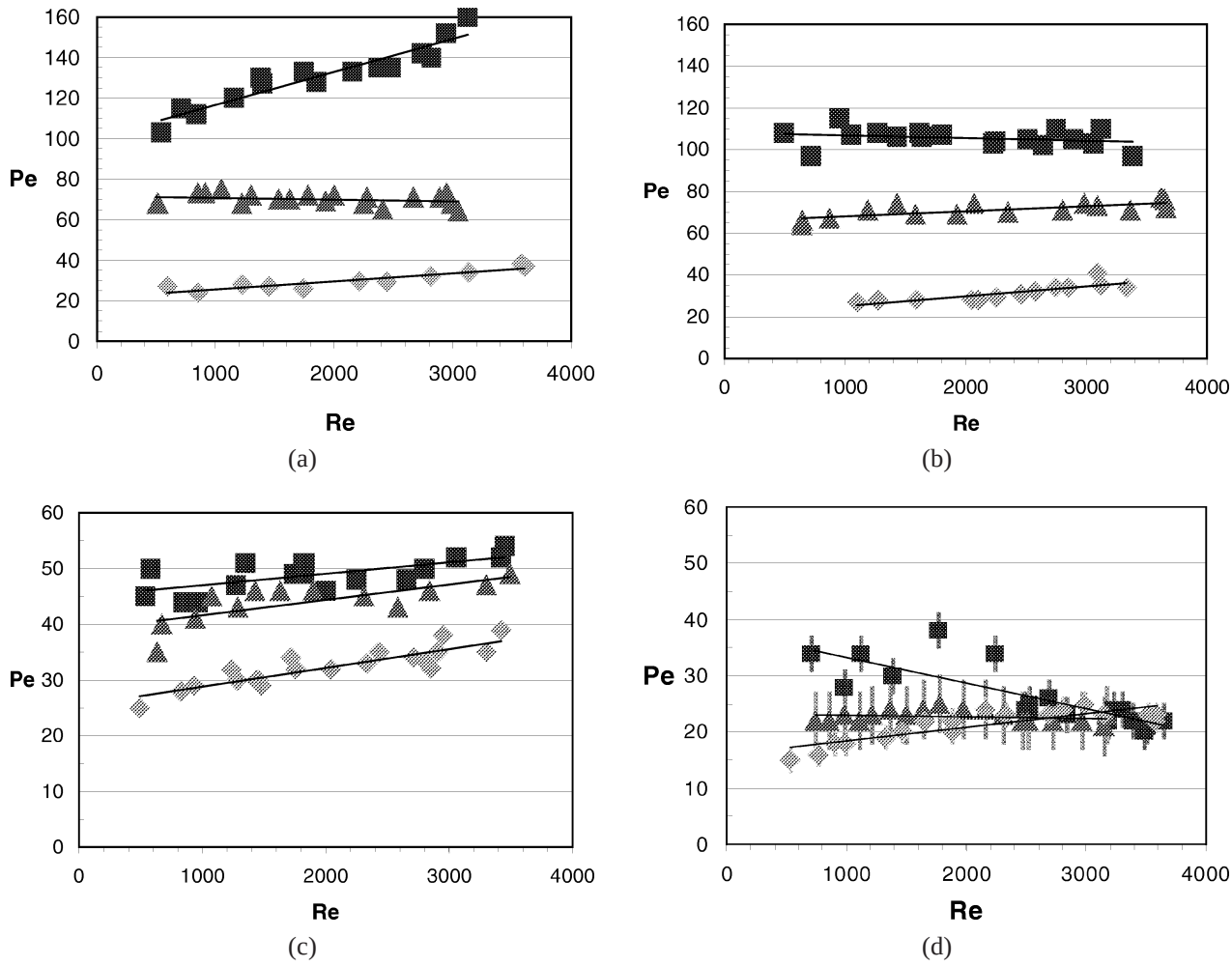

Figure 5. Péclet number versus Reynolds number for S&THE: (a) with 25 baffles, shell-to-baffle clearance: 0.2 mm (■), 1.0 mm (▲), 3.0 mm (♦); (b) with 17 baffles, shell-to-baffle clearance: 0.2 mm (■), 1.0 mm (▲), 3.0 mm (♦); (c) with 11 baffles, shell-to-baffle clearance: 0.2 mm (■), 1.0 mm (▲), 3.0 mm (♦); (d) with 7 baffles, shell-to-baffle clearance: 0.2 mm (■), 1.0 mm (▲), 3.0 mm (♦).

clearance and increasing the number of baffles. The width of the flow channel is decreased while the flow length is increased, and the flow is guided more stringently through the apparatus. The shortest and longest path through the exchanger as well as the highest and lowest travelling velocities deviate less from the mean with increasing number of baffles. This is, however, not really true for the configurations with relatively large shell-to-baffle clearance of 3.0 mm. *Figure 6* shows no significant difference between configurations with 11, 17, and 25 baffles for the Péclet number at equal axial plug flow Reynolds numbers. Reducing the number of baffles to 7, however, leads to a decrease of the Péclet number for the whole range of the Reynolds number. In this case the amount of dispersion is mostly determined by the large spacing of the baffles, which reduces the Péclet number already to lower values even for small shell-to-baffle clearances.

Figure 7 summarizes qualitatively the effects of baffle spacing and shell-to-baffle clearance for $Re = 2\,500$. While for negligible clearance dispersion decreases significantly with the spacing of the baffles, a large enough clearance of 3.0 mm basically eliminates the influence of baffle spacing. Looking at it from the viewpoint of the installed number of baffles, the influence of the clearance becomes significant when it disappears. Trying to reduce dispersion by avoiding shell-to-baffle clearance is useful only with an adequate number of baffles. Increasing the

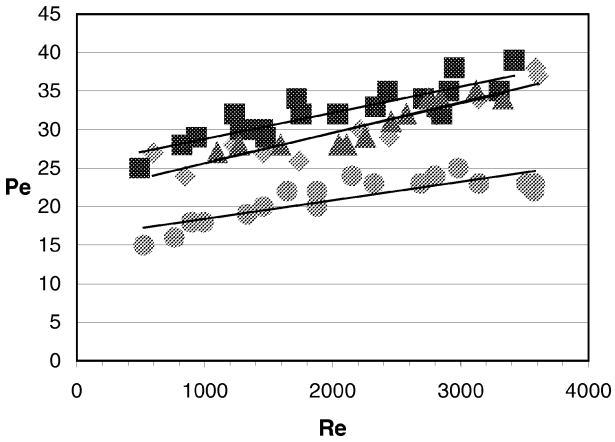

Figure 6. Péclet number versus Reynolds number for S&THE shell-to-baffle clearance 3.0 mm, number of baffles: 25 (♦), 17 (▲), 11 (■), 7 (●).

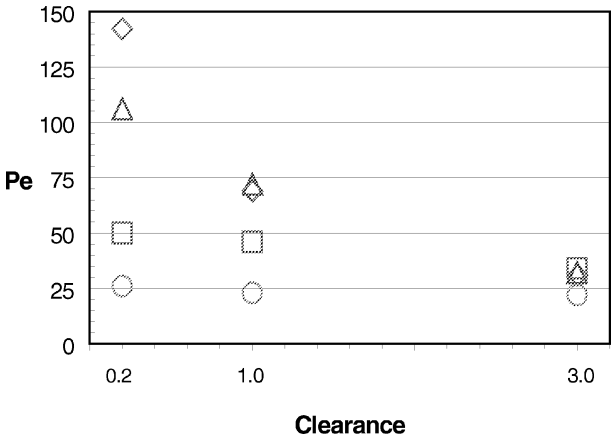

Figure 7. Péclet number versus shell-to-baffle clearance in the S&THE, $Re = 2500$, number of baffles: 25 (♦), 17 (▲), 11 (■), 7 (●).

number of baffles to aim at smaller dispersion will only be successful if sufficiently small shell-to-baffle clearance can be assured.

5. CONCLUSIONS

The shell-side dispersive Péclet number can change significantly with shell-to-baffle clearance, number of baffles and axial plug flow Reynolds number *Re*. Changes from $Pe = 15$ to 160 were detected. The highest value of *Pe* occurs with highest number of baffles at the highest Reynolds number and smallest shell-to-baffle clearance. The lowest value of *Pe* occurs with the lowest number of baffles, lowest Reynolds number and largest clearance.

The Péclet number depends mainly on the geometry, however, it may have a remarkable dependence on the Reynolds number.

For a given heat exchanger the dependence of the Péclet number on the Reynolds number is a monotonic function. Therefore, two or three measurements at different Reynolds numbers may be sufficient to describe the dispersive behaviour.

As the changes in *Pe* are strong, the axial dispersion model appears to be necessary for the prediction of transient processes in shell-and-tube heat exchangers.

The large variety of possible influences of geometry on axial dispersion suggest experimental determination for each geometry of concern rather than evaluation of empirical relationships or numerical simulations. Since the exact values of sensitive data like the shell-to-baffle clearance are often unknown, other methods than measurements could lead to greater errors in quantifying axial dispersion.

Measurements on the tube side should also be carried out in order to detect maldistribution inside the bundle.

REFERENCES

[1] Tinker T., Shell side characteristics of segmentally baffled shell-and-tube heat exchangers, Parts I, II, and III, in: Proceedings of General Discussion on Heat Transfer, ImechE, London, 1951, pp. 89–116.

[2] Pekdemir T., Davies T.W., Haseler L.E., Diaper A.D., Flow distribution on the shell-side of a shell-and-tube heat exchanger, Int. J. Heat Fluid Flow, Vol. 14 (1) (1993) 76–85.

[3] Taylor S.G., The dispersion of matter in turbulent flow through a pipe, Proc. Roy. Soc. London, Ser. A 223 (1954) 446–468.

[4] Roetzel W., Spang B., Effective mean temperature difference in segmentally baffled shell-and-tube heat exchangers, in: Proceedings of the 9th International Heat Transfer Conference, Vol. 5, Jerusalem, Israel, August 19–24, 1990, 14-HX-14, pp. 79–84.

[5] Spang, B., Über das thermische Verhalten von Rohrbündelwärmeübertragern mit Segmentumlenkblechen, Fortschr.-Ber. VDI, Reihe 19, Nr. 48, VDI-Verlag, Düsseldorf, 1991.

[6] Roetzel W., Transient analysis in heat exchangers, in: Afgan N. et al. (Eds.), New Developments in Heat Exchangers, Gordon & Breach, Amsterdam, 1996, pp. 547–575. Presented at the ICHMT International Symposium on New Developments in Heat Exchangers, Lisbon, 1993.

[7] Roetzel W., Xuan Y., Dynamic Behaviour of Heat Exchangers, WIT Press/Computational Mechanics Publications, Southampton, UK, 1999.

[8] Roetzel W., Luo X., Xuan Y., Measurement of heat transfer coefficient and axial dispersion coefficient using

temperature oscillations, Experimental Thermal and Fluid Science 7 (1993) 345–353.

[9] Roetzel W., Luo X., Extended temperature oscillation measurement technique for heat transfer and axial dispersion coefficients, Rev. Gén. Therm. 37 (1998) 277–283.

[10] Roetzel W., Balzereit F., Determination of axial dispersion coefficients in plate heat exchangers using residence time measurements, Rev. Gén. Therm. 36 (1997) 635–648.

[11] Köllmann K., Balzereit F., Meßverfahren zur zeitaufgelösten Konzentrationsbestimmung in strömenden elektrolytischen Flüssigkeiten, Technisches Messen 63 (1996) 458–464.

[12] Balzereit F., Bestimmung von axialen Dispersionskoeffizienten in Wärmeübertragern aus Verweilzeitmessungen, Fortschr.-Ber. VDI, Reihe 19, Nr. 48, VDI-Verlag, Düsseldorf, 1999.

[13] Danckwerts P.V., Continuous flow systems — distribution of residence times, Chem. Engrg. Sci. 2 (1953) 1–13.

[14] Roetzel W., Luo X., Pure cross-flow with longitudinal dispersion in one fluid, in: Shah R.K. et al. (Eds.), Aerospace Heat Exchanger Technology, Elsevier, 1993.

[15] Bracewell R.N., The Fourier Transform and its Application, 2nd edition, McGraw-Hill, New York, 1986.

[16] Spalding D.B., A note on mean residence times in steady flows of arbitrary complexity, Chem. Engrg. Sci. 9 (1958) 74–77.

[17] Prausnitz J.M., Wilhelm R.H., Turbulent concentration fluctuations through electrical conductivity measurements, The Review of Scientific Instruments 27 (11) (1956) 941–943.

[18] Khang S.J., Fitzgerald T.J., A new probe and circuit for measuring electrolyte conductivity, Ind. Eng. Chem. Fundam. 14 (1975) 208–213.